

## Microcolumn studies of dye adsorption onto manganese oxides modified diatomite

M.A. Al-Ghouti<sup>a,\*</sup>, M.A.M. Khraisheh<sup>b</sup>, M.N. Ahmad<sup>c</sup>, S.J. Allen<sup>c</sup>

<sup>a</sup> Royal Scientific Society, Industrial Chemistry Centre, P.O. Box 1438, Al-Jubaiha 11941, Jordan

<sup>b</sup> Department of Civil and Environmental Engineering, University College London, Chadwick Building, Gower Street, London WC1E 6BT, UK

<sup>c</sup> School of Chemistry and Chemical Engineering, Queen's University Belfast, David Keir Building, Stranmillis Road, Belfast BT9 5AG, Northern Ireland, UK

Received 6 August 2006; received in revised form 10 December 2006; accepted 12 December 2006

Available online 15 December 2006

### Abstract

The method described here cannot fully replace the analysis of large columns by small test columns (microcolumns). The procedure, however, is suitable for speeding up the determination of adsorption parameters of dye onto the adsorbent and for speeding up the initial screening of a large adsorbent collection that can be tedious if a several adsorbents and adsorption conditions must be tested. The performance of methylene blue (MB), a basic dye, Cibacron reactive black (RB) and Cibacron reactive yellow (RY) was predicted in this way and the influence of initial dye concentration and other adsorption conditions on the adsorption behaviour were demonstrated.

On the basis of the experimental results, it can be concluded that the adsorption of RY onto manganese oxides modified diatomite (MOMD) exhibited a characteristic “S” shape and can be simulated effectively by the Thomas model. It is shown that the adsorption capacity increased as the initial dye concentration increased. The increase in the dye uptake capacity with the increase of the adsorbent mass in the column was due to the increase in the surface area of adsorbent, which provided more binding sites for the adsorption. It is shown that the use of high flow rates reduced the time that RY in the solution is in contact with the MOMD, thus allowing less time for adsorption to occur, leading to an early breakthrough of RY. A rapid decrease in the column adsorption capacity with an increase in particle size with an average 56% reduction in capacity resulting from an increase in the particle size from 106–250  $\mu\text{m}$  to 250–500  $\mu\text{m}$ .

The experimental data correlated well with calculated data using the Thomas equation and the bed depth–service time (BDST) equation. Therefore, it might be concluded that the Thomas equation and the BDST equations can produce accurate prediction for variation of dye concentration, mass of the adsorbent, flow rate and particle size. In general, the values of adsorption isotherm capacity obtained in a batch system show the maximum values and are considerably higher than those obtained in a fixed-bed.

© 2006 Elsevier B.V. All rights reserved.

**Keywords:** Diatomite; Modified diatomite; Microcolumn; Reactive dyes; Textile effluent; Adsorption

### 1. Introduction

The disposal of textile wastewater effluents has become an important factor in running factories in many industries, and attention has to be given to methods of dealing with wastewaters in order to select the most economical methods [1,2]. There is growing interest in using low cost, commercially available materials for the adsorption of dyes. Diatomite, a siliceous sedimentary rock available in abundance in various locations around the world, has received attention for its unique combination of

physical and chemical properties (such as high permeability, high porosity, small particle size, large surface area, low thermal conductivity and chemical inertness) and as low cost material for the removal of pollutants from wastewater [3]. Previous studies by the authors established that chemical modification of diatomite, especially with manganese oxides (manganese oxides modified diatomite (MOMD)), enhanced its dye removal capacity and its feasibility for large-scale application to the treatment of textile effluents containing reactive dyes; a difficult class of dyes to treat in traditional methods. Detailed information about the effect of this chemical modification can be found in reference [4]. Other modifications have also been done by the authors such as microemulsion modified diatomite. This modification was not highly effective in reactive dye removing. But it was an excellent

\* Corresponding author. Tel.: +962 65344701; fax: +962 65344806.  
E-mail address: [mghouti@rss.gov.jo](mailto:mghouti@rss.gov.jo) (M.A. Al-Ghouti).

### Nomenclature

$a$	the slope
$b$	the intercept of the equation
$C$	the initial dye concentration (mg/L)
$C_b$	the breakthrough dye concentration (mg/L)
$C_t$	the equilibrium concentration (mg/L) at time $t$ (min)
$F$	the flow rate (L/min)
$k_T$	the Thomas constant (L/min mg)
$K$	the adsorption rate constant (L/g min)
$m$	the mass of adsorbent (g)
$N_0$	the column adsorption capacity in BDST model (g/L)
$q$	the maximum column adsorption capacity (mg/g)
$V$	the throughput volume (L)
$Z$	the bed depth (dm)

one for methylene blue removing. Moore and Reid [5] showed that manganese-impregnated acrylic fibres were effective for removing radium from natural waters. Khraisheh et al. [6] also showed the effectiveness of removal of  $Pb^{2+}$ ,  $Cu^{2+}$  and  $Cd^{2+}$  ions from wastewater using manganese modified diatomite. De Castro Dantas et al. [7] studied the removal of cadmium from aqueous solutions by diatomite with microemulsion.

Here, column studies are carried out to investigate the adsorption behaviour of dye adsorption onto the adsorbent. Batch type process is usually limited to the treatment of small volumes of effluents, whereas the bed column system has the advantage of operating continuous. For application of activated carbon adsorption in advanced water and wastewater treatment, the fixed-bed adsorber is considered most efficient [1]. Column studies could be conducted using large and small-scale columns. In this paper, it also has been decided to use a microcolumn to investigate the adsorption parameters and compare the results with those of large column. Furthermore, studying the adsorption process of a material using the microcolumn gives quick results. It is worthwhile mentioning here that large column studies give accurate results of the adsorption systems [8]. However, it has been suggested that the microcolumn technique could satisfactorily simulate the bed performance for large column runs [1].

Diatomite, as an adsorbent, can effectively remove the basic dye from solution and is inexpensive [4]. The capability of diatomite to remove reactive dyes from aqueous solution is less efficient compared to activated carbon [4]. In addition, when diatomite is directly used in wastewater treatment, there are some limitations, especially in column studies, especially in relation to low filtration rate. Al-Ghouti et al. [3] and Khraisheh et al. [4] showed that MOMD is a much more effective adsorbent for the removal of basic and reactive dyes from aqueous solutions. As a result, in this paper, MOMD was used as the main adsorbent. It has also been shown that MOMD has a high selectivity for dye removal.

Once the adsorbent has been chosen, the next important step is to conduct adsorption column tests and to investigate the column performance subject to different experimental conditions. In investigation of the column adsorption for removing the dye, two types of column experiments were conducted, small (microcolumn) and large (macrocolumn) columns. To our knowledge there is no research in the literature related to the use of microcolumns connected to a detector (spectrophotometer) in the study of the adsorption behaviour of dye onto adsorbent. Therefore, a rapid method for determining the adsorption parameters of dye onto MOMD for microcolumn application is proposed here.

Two simple mathematical models have been applied for the experimental data to predict the dynamic behaviour of the column and the following models characterising fixed-bed performance are discussed in detail here.

#### 1.1. Thomas model

Thomas derived the mathematical expression for a column with a typical breakthrough curve [9]

$$\frac{C_t}{C_0} = \frac{1}{1 + \exp [k_T(q_0m - C_0V)/F]} \quad (1)$$

$$\Rightarrow \ln \left( \frac{C_0}{C_t} - 1 \right) = \frac{k_T q_0 m}{F} - \frac{k_T C_0}{F} V \quad (2)$$

where  $C_0$  is the initial dye concentration (mg/L),  $C_t$  is the equilibrium concentration (mg/L) at time  $t$  (min),  $k_T$  is the Thomas constant (L/min mg),  $F$  is the volumetric flow rate (L/min),  $q_0$  is the maximum column adsorption capacity (mg/g),  $m$  is the mass of adsorbent (g) and  $V$  is the throughput volume (L).

Hence, a plot of  $\ln(C_0/C_t - 1)$  versus  $V$  gives a straight line with a slope of  $(-k_T C_0/F)$  and an intercept of  $(k_T q_0 m/F)$ . Therefore,  $k_T$  and  $q_0$  can be obtained.

#### 1.2. Bed depth–service time model (BDST)

The linear relationship between bed depth,  $Z$ , and service time,  $t$ , is [10]:

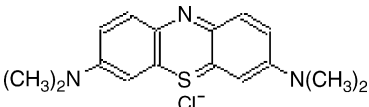
$$\ln \left( \frac{C_0}{C_b} - 1 \right) = \ln(e^{K_a N_0 Z/F} - 1) - K_a C_0 t \quad (3)$$

Because the exponential term,  $e^{K_a N_0 Z/F}$ , is usually much higher than unity, the unity term within the brackets on the left-hand side of equation is often neglected [10]. Therefore, the linear relationship between the bed depth,  $Z$ , and the service time at breakthrough,  $t_B$ , is:

$$t_B = \left( \frac{N_0}{C_0 F} \right) Z - \frac{1}{K_a C_0} \ln \left( \frac{C_0}{C_b} - 1 \right) \Rightarrow t_B = aZ + b \quad (4)$$

where  $C_0$  is the initial dye concentration (mg/L),  $C_b$  is the breakthrough dye concentration (mg/L),  $Z$  is the bed depth (dm),  $N_0$  is the column adsorption capacity in BDST model (g/L),  $F$  is the flow rate (L/min),  $K_a$  is the adsorption rate constant (L/g min),  $a$  is the slope and  $b$  is the intercept of the equation.

Table 1  
Main characteristics of the dyes used in this study

	Dye		
	MB	RB	RY
Type	Basic dye C.I. 52015	Cibacron reactive black C-NN	Cibacron reactive golden yellow MI-2RN
Phase	Solid	Liquid, 33 wt%	Liquid, 33 wt%
$\lambda_{\max}$ (nm)	663	597	430
$\varepsilon$ (dm <sup>3</sup> g <sup>-1</sup> cm <sup>-1</sup> )	170.1	22.6	23.0
Chemical structure	$C_{16}H_{18}N_3S^+Cl^-$ 	Unknown	Unknown

## 2. Materials and methods

Diatomite samples were obtained from borehole BT-36, depth 34–36 m in Al-Azraq region in East Jordan. Methylene blue (MB), a basic dye, Cibacron reactive black (RB) and Cibacron reactive yellow (RY) dyes were used; a summary of the main characteristics of these dyes is given in Table 1. The standard stock solutions of the dyes were prepared by appropriate dilution with deionised water to a final concentration of 1000 mg/L. To represent real textile effluent conditions, the reactive dyes were hydrolysed using the method described by Laszlo [11].

The diatomite was modified by treatment with manganese chloride and sodium hydroxide. The details of the preparation are given elsewhere [3]. The column tests were carried out in a micro-glass column with inside diameter of 3.35 mm and length of 7 cm. The microcolumns were randomly filled with MOMD samples. Air pockets form in the column could lead to channeling, increase in pressure drop and premature breakthrough due to the air pockets reducing the surface available for mass transfer between the MOMD and the dye solution. To solve this problem [10], deionised water was used to wash the MOMD sample in order to remove air bubbles and to rinse the MOMD. After a designated amount of dry MOMD particles was filled in the microcolumn, microcolumn was then immersed in a glass beaker containing deionised water and sucked for about 15 min with a vacuum pump to eliminate air pockets form in the column. Moreover, dye solution with different concentrations was continuously fed to the top of the column at various flow rate controlled by a peristaltic pump (Watson-Marlow, 101U) connected with Teflon tubes to the column inlet until breakthrough occurs. Column outlet was connected with flow cell of spectrophotometer by Teflon tubes. Absorbance readings were taken every 40 s. A stock solution of MB, RB and RY was prepared by dissolving 1000 mg/L in deionised water. Different dye concentrations, 60, 80, 100, and 150 mg/L were prepared. Before starting the adsorption tests, the system was checked by circulating water and the dye concentration was measured by passing the initial dye concentration through the flow cell. Duplicate samples were measured and the standard error in the readings was less than 5%. Fig. 1 illustrates a schematic representation of microcolumn adsorption onto MOMD. The main components

are: (i) peristaltic pump, (ii) microcolumn, (iii) Teflon tubes, (iv) mixer, (v) flow cell and (vi) UV-Vis spectroscopy.

Further experiments studying the effect of initial dye concentration, mass of adsorbent, flow rate, internal diameter and particle size, were also considered. RY was chosen as a model system in these experiments. Details of experimental conditions of the microcolumn studies of RY onto MOMD for all the microcolumn runs undertaken are listed in Table 2. In order to study the affinity of reactive dyes for MOMD in the microcolumn studies, pure and binary adsorption experiments were also carried out. Experiments were carried out using macrocolumn (large column) to evaluate the adsorption parameters and to compare the result with those of microcolumn. Macrocolumn studies were performed by using a burette glassy column (50 mL) and the columns were kept in vertical position. A known amount of the dye concentration was added to a beaker (2 L) to hold the dye solution, and it was kept under continuous stirring by means of a glass rod. Samples were collected in cuvettes continuously for each experiment by fraction collector, and analysed regularly to

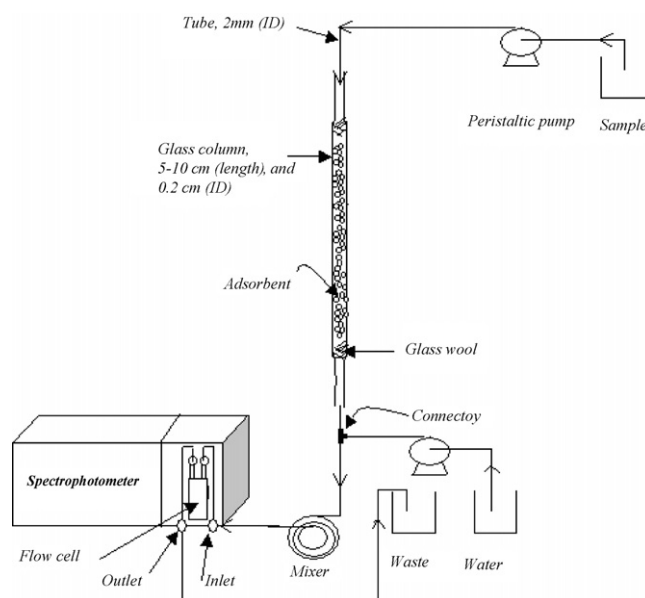


Fig. 1. Schematic representation of microcolumn adsorption of the dyes onto MOMD.

Table 2

Experimental conditions of the various microcolumn adsorption experiments for the removal of RY onto MOMD

Parameter	Initial dye concentration (mg/L)	Mass of adsorbent (g)	Flow rate (mL/min)	Particle size ( $\mu\text{m}$ )	Internal diameter (mm)
Initial dye concentration (mg/L)	57, 79, 101, 149	0.4	3.77	106–250	3.35
Mass of adsorbent (g)	57	0.1, 0.2, 0.3, 0.4	6.82	106–250	3.35
Flow rate (mL/min)	57	0.4	1.60, 2.35, 3.77, 5.19, 6.82	106–250	3.35
Particle size ( $\mu\text{m}$ )	57	0.4	3.77	106–250, 250–500	3.35
Internal diameter (mm)	57	0.4	3.77	106–250	2.25, 3.35, 4.95

Table 3

Experimental conditions of the various macrocolumn adsorption experiments for the removal of RY and MB onto MOMD

Experimental conditions	
Adsorbent	MOMD
Adsorbate	MB and RY
Initial dye concentration (mg/L)	50
Particle diameter ( $\mu\text{m}$ )	106–250
Mass of MOMD (g)	1.0
Flow rate (mL/min)	3.77
Column internal diameter (cm)	1.10
Temperature ( $^{\circ}\text{C}$ )	22

monitor the dye concentration leaving the column. This was continued until the concentration of dye leaving the column was very close to the feed. The final dye concentrations were determined using a Perkin-Elmer UV-Vis spectrophotometer corresponding to  $\lambda_{\text{max}}$  of each dye. The experimental conditions of dye adsorption onto MOMD using macrocolumn were illustrated in Table 3.

### 3. Results and discussion

The experimental adsorption data from the microcolumn studies was analysed using the Thomas equation. Application of the Thomas model to the data at  $C_i/C_0$  ratios higher than 0.05 and lower than 0.90 with respect to the adsorption conditions such as flow rate, dye concentration, particle size, mass of adsorbent and column internal diameter enabled the determination of the adsorption parameters of the system. The description of the column performance has also been based on the bed depth–service time (BDST) model of Bohart and Adams [12].

The slope and intercept of the Thomas equation is dependent on three parameters: the initial dye concentration, mass of adsorbent used and the volumetric flow rate. Moreover, the slope of the BDST equation is dependent on the initial dye concentration, flow rate and adsorption capacity. However, as the cross-section area of the column is kept constant throughout all experiments and the flow rates is also constant, then the only cause of the change in slope is due to the bed capacity [13].

In the column studies, RY was chosen as a model system for the dye removal from aqueous solution due to its high adsorption kinetics. Then, the optimised parameters from this system were applied for RB and MB adsorption. The behaviour of adsorption of RY molecules onto MOMD was studied in microcolumn experiments. The microcolumn (small column) experimental results could predict the adsorption parameters for

large columns. In order to study the affinity of reactive dye for MOMD in the column studies, single and binary adsorption experiments were also carried out. Real effluents contain not only the single adsorbate, but also other pollutants, which could exert influence the adsorption behaviour.

For most adsorption operations in wastewater treatments, breakthrough curves exhibit a characteristic “S” shape [14]. Various factors could affect the actual shape of the curve such as initial dye concentration, mass of adsorbent, particle size, flow rate and pH [14]. Furthermore, the general position of the breakthrough curve along the volume axis depends on the capacity of the column with respect to these factors. These factors will be discussed in the following subsections.

#### 3.1. Column studies of adsorption of reactive yellow (RY) onto MOMD

##### 3.1.1. Effect of initial dye concentration

The effect of initial dye concentration on the shape of the breakthrough curves and the column adsorption parameters was investigated. Fig. 2 depicts the breakthrough curves of adsorption of RY onto MOMD at different initial dye concentrations as a plot of dimensionless concentration ( $C_t/C_0$ ) versus volume ( $V$ ) of dye treated. It can be seen from Fig. 2 that the shape of the breakthrough curves of adsorption of RY at various initial dye concentrations exhibited a characteristic “S” shape. The initial dye concentration is important since a given mass of MOMD can only adsorb a certain amount of the dye. Consequently, the more concentrated the solution, the smaller is the volume of the solu-

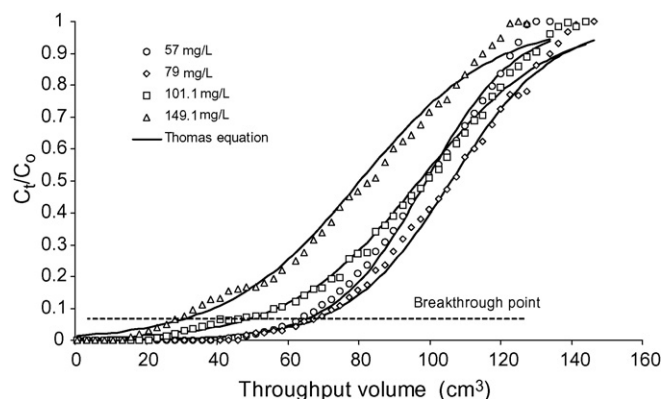


Fig. 2. Breakthrough curve of adsorption of RY onto MOMD using microcolumn at different initial dye concentrations. Experimental conditions: mass of MOMD, 0.4 g; particle size, 106–250  $\mu\text{m}$ ; internal diameter, 3.35 mm; flow rate, 3.77 mL/min; pH 2; temperature: 21  $^{\circ}\text{C}$ .

Table 4

Thomas parameters of adsorption of RY onto MOMD at different initial dye concentration, mass of adsorbent, flow rate, particle size distribution and internal diameter

	Parameter		$R^2$
	$k_T/10^{-3}$ (L/min mg)	$q_0$ (mg/g)	
Initial dye concentration (mg/L)			
57.0	5.19	14.12	0.9907
79.0	3.30	20.96	0.9955
101.1	2.04	24.58	0.9891
149.1	1.34	30.02	0.9848
Mass of adsorbent (g)			
0.1	22.7	5.494	0.9860
0.2	22.3	7.041	0.9930
0.3	13.5	8.770	0.9985
0.4	10.1	10.10	0.9984
Flow rate (mL/min)			
6.82	10.1	10.10	0.9984
5.19	7.51	12.08	0.9941
3.77	5.19	14.12	0.9907
2.35	2.87	17.31	0.9937
1.60	1.78	18.33	0.9872
Particle size distribution ( $\mu\text{m}$ )			
106–250	5.19	14.12	0.9907
250–500	7.45	6.261	0.9877
Internal diameter (mm)			
2.25	6.66	11.33	0.9890
3.35	5.19	14.12	0.9907
4.95	3.40	17.37	0.8746

tion that can be treated [14]. The Thomas equation was used to estimate the column adsorption parameters and the results are shown in Table 4. It is shown that the adsorption capacity increased as the initial dye concentration increased. This is due to the concentration gradient. Higher initial dye concentrations lead to a higher concentration gradient hence the mass transfer driving force will be higher [15]. Table 4 also shows that the rate constant,  $k_T$ , decreases as the initial dye concentration increases. The increase of RY concentration results in an increase the in driving force, which will enhance the diffusion rate of the molecular dye in pores. The breakthrough point time decreased with increasing inlet RY concentration as the binding sites became quickly saturated in the system (Aksu and Gönen [13]). For example, the breakthrough point ( $C_t/C_0=0.05$ ) occurred after 6 min (corresponding to 22 mL of dye effluent) at 149.1 mg/L RY concentration, while breakthrough point appeared after 16 min (corresponding to 62 mL of dye effluent) at an inlet dye concentration of 57 mg/L.

Walker and Weatherley studied the adsorption of acid dyes onto activated carbon using fixed-bed columns [10]. It was shown that increasing inlet dye concentration at constant flow rate decreased the throughput volume until breakthrough. This may be due to high dye concentrations saturating the adsorbent more quickly, as a result, decreasing the breakthrough time. Breakthrough curves calculated from the Thomas equation using the fitted  $k_T$  and  $q_0$  values are shown as curves in Fig. 2, in comparison with the experimental data. Overall, the experimental

data are well presented by the Thomas equation over a wide range of the dye concentration. It is also clear that the experimental data did not fit well with the Thomas equation when  $C_t/C_0$  ratio was greater than 0.8. The deviation of the Thomas model predictions at the later stage of the breakthrough curves is probably because that the Thomas model assumes Langmuir kinetics of adsorption-desorption and no axial dispersion is derived with the adsorption and that the rate driving force obeys second-order reversible reaction kinetics. It was shown in Al-Ghouti et al. [3] that the adsorption process of RY onto MOMD obeyed the pseudo-second order reaction but external and intraparticle diffusion also played a role in the adsorption process. Therefore, the Thomas model is suitable for adsorption processes where the external and internal diffusion will not be the limiting step [13].

### 3.1.2. Effect of mass of adsorbent

The observed breakthrough curves of RY for MOMD at four different masses of adsorbent are displayed in Fig. 3, plotted as the effluent concentration ratio versus the throughput volume. It is clear from Fig. 3 that the shape of the breakthrough curves, at various mass of MOMD, is different. The time needed to reach the breakthrough point is lower for 0.1 g MOMD. The uptake of RY increased with the increase in MOMD mass from 0.1 to 0.4 g. The increase in the dye uptake capacity with the increase of the adsorbent mass in the column was due to the increase in the surface area of adsorbent, which provided more binding sites for adsorption [12].

As indicated in Fig. 3, at the lowest mass of adsorbent, that is 0.1 g, a relatively lower uptake value was observed for RY adsorption at the beginning of column adsorption. In addition, as dye solution continued to flow, the RY concentration in the effluent rapidly increased, the bed became saturated with RY molecules and the dye concentration in the effluent suddenly rose to the inlet RY concentration. Less sharp breakthrough curves were obtained at higher mass of adsorbent. The variation in breakthrough shape with MOMD mass is mainly due to the relatively large adsorption zone, that is MOMD near the bot-

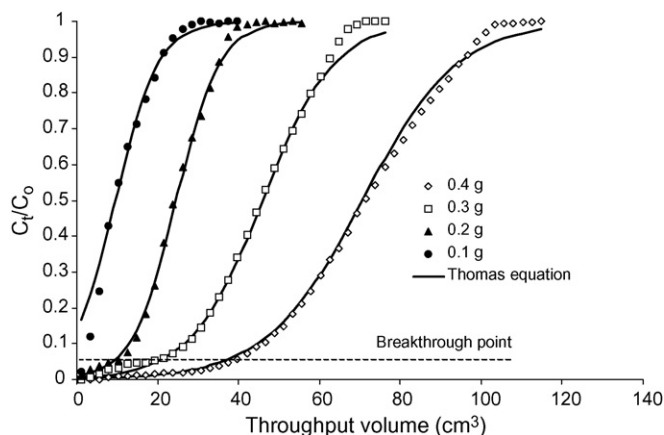


Fig. 3. Breakthrough curve of adsorption of RY onto MOMD using micro-column at various masses of MOMD. Experimental conditions: initial reactive dye concentration, 57.24 mg/L; particle size, 106–250  $\mu\text{m}$ ; internal diameter, 3.35 mm; flow rate, 6.82 mL/min; pH 2; temperature, 21  $^{\circ}\text{C}$ .

Table 5  
BDST data for RY adsorption onto MOMD

Bed depth (dm)	Service time at breakthrough for percentage removals (min)				BDST equation simplified as ( $t_B = aZ + b$ )	$N_0$ (g/L)	$N_0$ (mg/g) <sup>a</sup>	$K_a$ (L/g min) ( $10^{-3}$ ) <sup>b</sup>
	20%	40%	60%	80%				
0.14	0.75	1.13	1.67	2.63	20% $\Rightarrow t_B = 19.6Z - 2.56$	8.679	10.71	9.81
0.28	2.08	3.25	3.87	4.80	40% $\Rightarrow t_B = 23.1Z - 2.59$	10.25	12.65	2.66
0.39	5.00	6.17	7.30	8.53	60% $\Rightarrow t_B = 24.4Z - 2.46$	11.29	12.95	—
0.52	8.00	9.83	11.2	13.0	80% $\Rightarrow t_B = 27.7Z - 1.98$	12.25	14.05	—

<sup>a</sup>  $N_0$  (mg/g) was calculated by multiplying the value of  $N_0$  (g/L) by the apparent bulk density [ $m/((\pi r^2) \times L)$ ].

<sup>b</sup> Values  $K_a$  did not compute for 60 and 80% breakthrough due to their negative values.

tom of the adsorption column, which comes into contact with dye solution after MOMD near the top of column, is exhausted. The rate at which the adsorption zone travels through the column decreases with the MOMD bed depth, indicating that beds of increased heights may be required for dye adsorption [10]. Therefore, the mass transfer zone (MTZ) has its own characteristics that are dependent upon the nature of adsorbent-adsorbate interactions in addition to the experimental conditions such as mass of adsorbent, initial dye concentration, etc.

Fig. 3 shows that the breakthrough curves shifted towards the origin with decreasing mass of adsorbent. Fig. 3 also indicates that the breakthrough curves, except for 0.1 g MOMD, do follow the characteristic “S” shape profile produced in an ideal adsorption system. Furthermore, it may be seen that the experimental results is in a good agreement with the Thomas equation at different masses of adsorbent, 0.1 and 0.2 g MOMD in particular. The column adsorption parameters of RY adsorption are shown in Table 5. To predict the mass of MOMD that might be needed to get higher adsorption capacity, similar to the equilibrium adsorption ones, a plot of mass of adsorbent versus column adsorption capacity,  $q_0$ , was drawn and the estimated mass found to be around 13 g MOMD.

The analysis of the experimental breakthrough data, using the BDST equation, yielded a plot of bed depth,  $Z$ , versus service time,  $t_B$ , illustrated in Fig. 4. The linearisation of the experimental data using this technique proved quite successful for the adsorption of RY onto MOMD ( $R^2 = 0.97$ ). However, a close examination of the straight lines in Fig. 4 suggests that the experimental points of the BDST, deviate from a theoretical straight line and the correlation coefficient, was around 0.97.

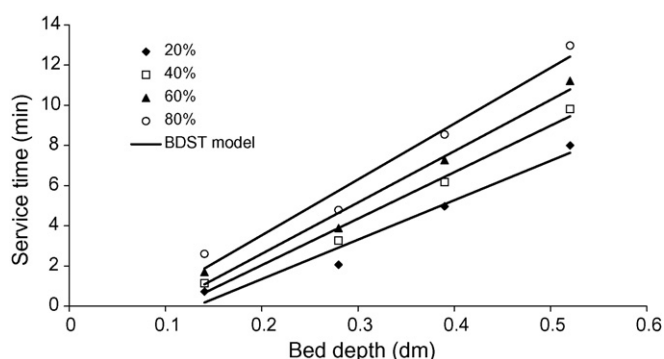


Fig. 4. Plots of bed depth ( $Z$ ) vs. service time ( $t_B$ ) at different percentage breakthrough points.

This behaviour may be due to the fact that the dye–MOMD system has a strange diffusional resistance, such that the traditional BDST model cannot be applied successfully. The main assumption in the BDST approach is that the adsorbate is adsorbed on the adsorbent surface immediately such that there is no diffusion problem [16]. Consequently, when the bed depth increases, the residence time of the dye solution inside the column increases and the dye molecules can diffuse deeper inside the adsorbent.

However, the main goal of operating a column adsorption system is to achieve a certain degree of reduction in the dye concentration, which may be called the percentage breakthrough value [12]. A small breakthrough value would mean having a small dye concentration in the effluent. Therefore, as  $C_b$  increases, the volume of dye liquid treated would be larger and the adsorber would run longer. The value of  $C_b$  should not affect the slope of the BDST plots, that is, the breakthrough curves are steep and the mass-transfer zone is very short [16]. In Table 5, BDST data represent the evolution of the bed running time (for different concentrations  $C_t = 20, 40, 60$  and  $80\%$ ) as a function of the bed depth ( $Z$ ). Based on the experimental data obtained at different masses of adsorbent for adsorption of RY onto MOMD, plotting time for 20, 40, 60 and 80% against bed height gives a linear relationship as seen in Fig. 4 with high correlation coefficients ( $R^2 > 0.97$ ). The BDST parameters, namely, BDST adsorption capacity,  $N_0$ , and rate constant,  $K_a$  were calculated from the linearised experimental data and are presented in Table 5, for 20, 40, 60 and 80% breakthrough. It is worth mentioning here that the value of  $N_0$ , calculated from the BDST equation, was divided by the cross-section area of the bed ( $\text{dm}^2$ ) to convert the unit of  $N_0$  from (g/dm) to (g/L). For each column, the material packing has to be the same in order to obtain the same apparent bulk density in each column. It is around  $\rho = 841$  g/L. Table 5 illustrates the effect of percentage breakthrough value on the adsorption capacity for the treatment for a fixed initial dye concentration of RY to final values of 20, 40, 60 and 80%. Furthermore, a small increase in the service times and the column adsorption capacities were achieved by altering the percentage breakthrough point, in particular at 0.52 dm bed depth, which may be due to the mass transfer zone (MTZ) is being short [12].

Table 5 shows that the column adsorption capacities, calculated by the Thomas equation, correlate well with the BDST equation (Table 5). The calculated column adsorption capacity by BDST is higher than that obtained by Thomas equation by 28%. Consequently, the Thomas equation is a useful tool

Table 6  
Column adsorption parameters of adsorption of RY, MB and RB onto MOMD

Dye	$k_T/10^{-3}$ (L/min mg)	$q_0$ (mg/g)	$R^2$	Equilibrium adsorption capacity (mg/g)	Fraction of equilibrium (%)	Batch adsorption capacity [3] (mg/g)
RY	5.19	14.12	0.9907	204	6.92	56.5
MB	3.38	13.56	0.9742	320	4.24	54.4
RB	1.87	17.17	0.9787	419	4.10	128

to predict the column adsorption capacity at various adsorption parameters such as dye concentration, flow rate, particle size and internal diameter. Comparing the experimental data in Table 6, it can be seen that the BDST equation applied to the data at 60 and 80% breakthrough gave a better adsorption capacity and a better approximation to the experimental results compared with 20% breakthrough point, as deviation from the theoretical value is much smaller. This behaviour was illustrated in Fig. 4, as the correlation coefficients at 60 and 80% breakthrough points are higher than at 20%.

It is clear that the experimental data correlated well with the calculated data using the Thomas and the BDST equation. Therefore, it might be concluded that the Thomas and the BDST equations can produce accurate prediction for variation of dye concentration, mass of the adsorbent, flow rate and particle size.

### 3.1.3. Effect of flow rate

In column studies contact time is the most significant variable and therefore bed depth and dye flow rate are the major parameters [17]. Consequently, adsorption of RY was studied at the flow rates of 6.8, 5.2, 3.8, 2.4 and 1.6 mL/min in order to investigate the effect of flow rate on the adsorption behaviour. Initial dye concentration, pH and particle size were maintained constant. The experimental results of the effect of flow rate are illustrated in Fig. 5. It is clearly shown that the breakthrough time increased with a decrease in the flow rate.

Fig. 5 shows that the uptake of RY decreases with the increase in flow rate. The results were illustrated in Table 4. For instance,

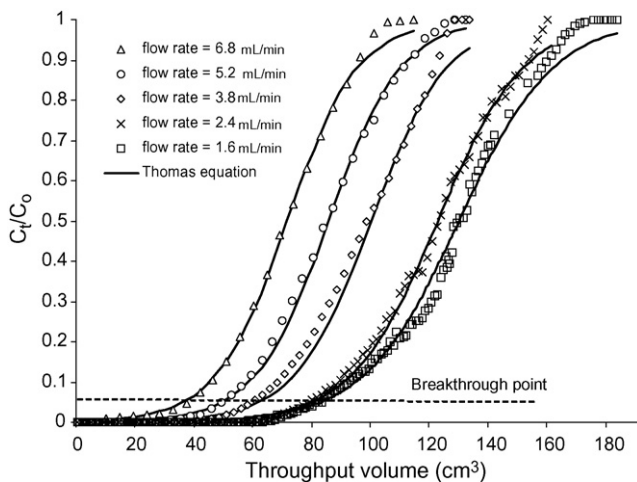


Fig. 5. Breakthrough curve of adsorption of RY onto MOMD using microcolumn at various flow rates. Experimental conditions: mass of MOMD, 0.40 g; initial RY concentration, 56.30 mg/L; internal diameter, 3.35 mm; particle size, 106–250  $\mu$ m; pH 2; temperature, 21 °C.

Zulfadhly et al. [18] observed a similar trend when investigating macro fungus *Pycnoporus sanguineus* to adsorb heavy metals (Pb, Cu and Cd) from aqueous solution in fixed-bed column at various flow rates. The experimental data in Fig. 5 shows that increasing the flow rate reduces the volume of the dye effluent treated at the breakthrough point. It is clearly shown that the adsorption capacity,  $q_0$ , increased as the flow rate decreased. The value of  $q_0$  changed from 10.10 to 18.33 mg/g when the flow rate changed from 6.82 to 1.6 mL/min. It is also shown that the Thomas rate constant increased as the flow rate increased. A large value of the rate constant indicates that the adsorption capacity will reach the equilibrium value faster. Furthermore, at the lower flow rate, there is longer adsorbent/dye contact time. However, the effect of flow rate on the adsorption capacity could be explained as: (i) a higher flow rate decreases the external film mass resistance at the surface of the adsorbent and (ii) the resistance time of the dye effluent inside the bed decreases with higher flow rate hence the time that is required to diffuse and penetrate into the centre of the adsorbent is lower [13,15]. The Thomas equation shows the slope is inversely proportional to the flow rate,  $F$  (slope  $\propto 1/F$ ) and the correlation coefficients ( $R^2$ ) values calculated for the linearisation of the experimental data were quite high with values all above 0.99.

The results show that a decrease in flow rate at a constant bed depth increased the throughput volume to breakthrough,  $V_B$ . The same behaviour was obtained by Chu [17]. It was shown that the use of high flow rates reduced the time that cadmium in the solution is in contact with the biomass, thus allowing less time for biosorption to occur, leading to an early breakthrough of cadmium. The results presented in Table 7 indicate that the adsorption process could deal with lower flow rates of dye solution if a high percentage removal is required. However, the use of low flow rate will result in long overall processing times which may not be desirable in practice when large volumes of dye-bearing wastewater have to be processed [17]. Careful examination of Fig. 5, in particular at low flow rates (2.35 and 1.60 mL/min), reveals that possible desorption might be occurring where the dye concentration appears to fluctuate. This behaviour could be attributed to either a reversible adsorption or a back diffusion controlling mechanism [19]. At high flow

Table 7  
Column adsorption parameters of adsorption of MB and RY onto MOMD using large column and microcolumn

Dye	$k_T/10^{-4}$ (L/min mg)	$q_0$ (large) (mg/g)	$R^2$	$q_0$ (small) (mg/g)
MB	2.97	17.25	0.9898	13.56
RY	6.31	26.44	0.9712	14.12

rates, the uptake removal was enhanced and desorption phenomena totally decreased. Consequently, by adjusting the operating conditions of the column such as flow rate, particle size, dye concentration, mass of adsorbent, and column internal diameter, the efficient dye uptake can be achieved for the adsorption system.

### 3.1.4. Effect of particle size

Another important parameter in the adsorption process is related to the particle size of the adsorbent. However, because of the pressure drop and the handling problems of the smaller particle sizes  $<106\ \mu\text{m}$  in the column studies, the particle sizes  $106\text{--}250\ \mu\text{m}$  and  $250\text{--}500\ \mu\text{m}$  were only used for the present column studies. Thus, the column adsorption studies on the RY were carried out on MOMD of particle sizes  $106\text{--}250\ \mu\text{m}$  and  $250\text{--}500\ \mu\text{m}$ . The breakthrough curves of the two particle size ranges are illustrated in Fig. 6. An increase in the particle size appeared to increase the sharpness of the breakthrough curve. Moreover, the Thomas equation was used to estimate the rate constant and the adsorption capacity of the system. Table 4 illustrates that the Thomas rate constant,  $k_T$ , increases with the increase in the mean adsorbent particle size. Furthermore, the adsorption capacity for the larger particle size is lower than that for smaller one. A rapid decrease in the column adsorption capacity with an increase in particle size with an average 56% reduction in capacity in addition to the clear shift of the breakthrough curve was obtained resulting from an increase in the particle size from  $106\text{--}250\ \mu\text{m}$  to  $250\text{--}500\ \mu\text{m}$ . That is mainly true due to the higher surface area of the smaller particle size hence a higher adsorption capacity is expected and also the mean intraparticle diffusion paths are shorter [20]. These results correlated well with the results from batch kinetic studies, in which the rate of dye adsorption appeared to increase with smaller particle size. Al-Ghouti et al. [4] showed also that the adsorption capacity of adsorption of RY onto MOMD increased with the reduced particle sizes. The same behaviour was also observed by Walker and Weatherley [10].

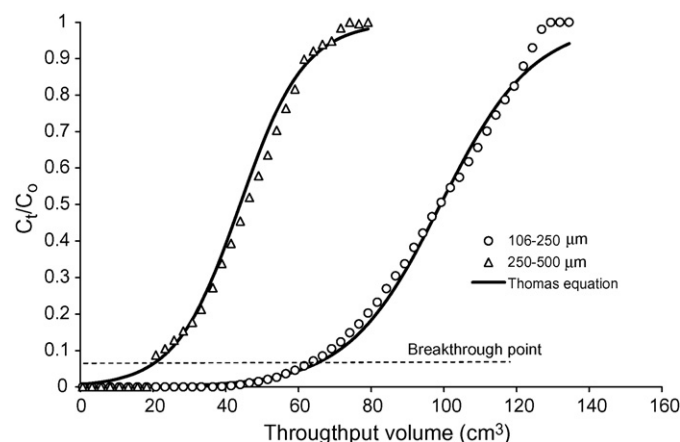


Fig. 6. Breakthrough curve of adsorption of RY onto MOMD using microcolumn at various particle sizes. Experimental conditions: mass of MOMD, 0.40 g; initial RY concentration, 56.30 mg/L; internal diameter, 3.35 mm; flow rate, 3.77 mL/min; pH 2; temperature, 21 °C.

It is clear from Fig. 6 that the experimental data for particle size  $250\text{--}500\ \mu\text{m}$  are well presented by the Thomas equation over the range (from 0 to  $1\ C_t/C_0$ ). The breakthrough curve of  $250\text{--}500\ \mu\text{m}$  particle size also exhibits a trailing edge. This behaviour is most likely due to slow intraparticle diffusion within the pores of the MOMD. A smaller particle size will have a faster pore diffusion rate because the diffusion path is shorter and the diffusion resistance is smaller [16]. This behaviour is correlated well with the results in which the intraparticle diffusion parameter is higher for smaller particle sizes [3].

It is interesting to point out that when the main dye adsorption process onto the adsorbent are those based on adsorption on the particle surface, higher dye adsorption is expected on smaller particles, as observed on MOMD [21]. Consequently, it can be concluded that the adsorption of RY onto MOMD was achieved on the particle surface.

### 3.1.5. Effect of internal diameter

Different internal diameters were chosen, 2.25, 3.35 and 4.95 mm, to investigate the effect of internal diameter on the adsorptive properties and the results are shown in Fig. 7. The major parameter for any adsorber system is the contact time. Due to the diffusion controlling nature of the dye adsorption onto MOMD a long contact time is required for the efficient use of the MOMD [3]. This can be achieved by two methods: (i) increasing the diameter of the column, and (ii) decreasing the volumetric flow rate,  $F$ , in the column [10]. The reported results in Table 4 revealed a difference in column performance in terms of column adsorption rate and adsorption capacity. Table 4 shows that as the internal diameter of the column increases from 2.25 to 4.95 mm, the adsorption capacity increases by 48%. This behaviour is to be expected. Moreover, the Thomas rate parameter,  $k_T$ , decreased from  $6.66 \times 10^{-3}$  to  $2.58 \times 10^{-3}$  L/min mg when the internal diameter increased from 2.25 to 4.95 mm and the shape of the breakthrough curves were slightly different with the variable internal diameters, 4.95 mm in particular. However, the breakthrough curve of the larger diameter (4.95 mm) tended to be more gradual. In fact, in the latter case, the breakthrough

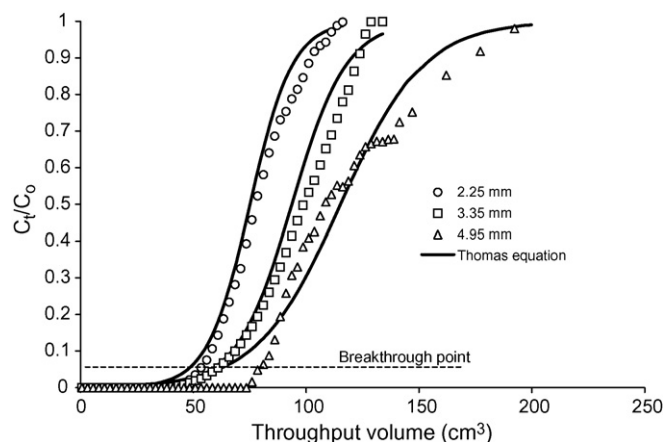


Fig. 7. Breakthrough curve of adsorption of RY onto MOMD using microcolumn at various internal diameters. Experimental conditions: mass of MOMD, 0.40 g; initial RY concentration, 60.30 mg/L; particle size,  $106\text{--}250\ \mu\text{m}$ ; flow rate, 3.77 mL/min; pH 2; temperature, 21 °C.



point occurred in approximately 20 min. For a smaller internal diameter of 2.25 mm, the breakthrough and saturation times were observed to be approximately 13 and 31 min, respectively. This shape of the breakthrough curve of the larger diameter showed that the system was not at equilibrium. The present shape attested that mass transfer limitations, probably through intraparticle diffusion, played a significant role [20]. To conclude, the different experimental parameters showed the nonequilibrium of RY adsorption in a column of MOMD. The breakthrough curve obtained at various experimental conditions (i.e. various particle sizes, flow rates, dye concentrations, etc.) were not conventional because these operating parameters had an influence not only on the breakthrough curve spreading but also on the RY adsorption. These observations enabled us to conclude that nonequilibrium was mainly due to intraparticle diffusion [20].

### 3.2. Adsorption of RB and MB

Various parameters including flow rate, initial dye concentration, particle size and mass of adsorbent was investigated for adsorption of RY onto MOMD. With the variation of the above parameters, the optimum conditions for the column operation can be obtained in order to apply these into the adsorption of MB and RB onto MOMD. Figs. 8 and 9 show the breakthrough curves of RB and MB, respectively. Comparison of the breakthrough curves for RY, MB and RB at a given bed height and flow rate show that these curves are quite different. This behaviour is to be expected, as the adsorption mechanism of each dye is different in addition to the variation in dye adsorption kinetics. From the experimental curves, it is also evident that, in order to saturate the MOMD, higher volumes of RB solution, contrast with, smaller volumes of MB and RY are necessary. It was evident that the predominant adsorption mechanism of RB is adsorption in the octahedral layers [22]. This could be explained in that the exhaustion point was not attained (maximum of 75%  $C_0$  effluent concentration after 50 mL). This feature seems to be related to the higher efficiency of MOMD material in removing RB compared with MB or RY. This behaviour could be explained by the adsorption mechanism. It also correlates well with the

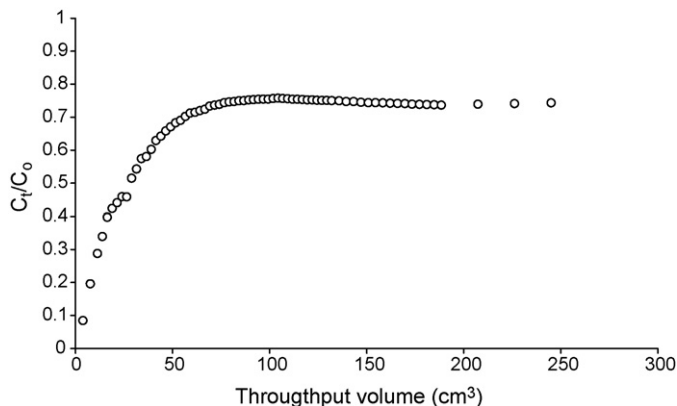


Fig. 8. Breakthrough curve of adsorption of RB onto MOMD using micro-column. Experimental conditions: mass of MOMD, 0.1 g; initial reactive dye concentration, 64.81 mg/L; flow rate, 3.77 mL/min; pH 2; particle size, 106–250  $\mu\text{m}$ ; temperature, 20 °C.

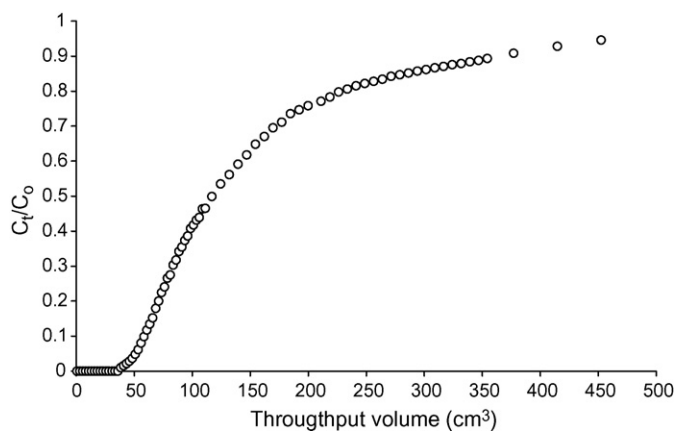


Fig. 9. Breakthrough curve of adsorption of MB onto MOMD using micro-column. Experimental conditions: mass of MOMD, 0.41 g; initial reactive dye concentration, 53 mg/L; flow rate, 3.77 mL/min; pH 11; particle size, 106–250  $\mu\text{m}$ ; temperature, 20 °C.

results in Al-Ghouti et al. [22] in which the main RB mechanism onto MOMD is by intercalation in the octahedral layers and the rate limiting-step might be intraparticle diffusion. The same behaviour was also obtained by Chu [17].

The MB breakthrough curve exhibits a smooth broad “S” shape with a quite rapid initial rise, followed by a gradual approach to the feed concentration (i.e. slow approach of  $C_t/C_0$  to 1). This is probably because intraparticle diffusion is playing an important role in the MB adsorption onto MOMD (i.e. intraparticle diffusion may be the rate limiting-step). The behaviour of MB adsorption onto MOMD could be explained as follows: when MB is passed through the MOMD column, the MB molecules readily adsorb on the modified diatomite particles. This adsorption occurred initially on the external surfaces and as result, a high concentration of MB molecules in this area increased considerably. It is known that for column operations, the adsorbent is continuously in contact with a fresh solution. Consequently, the stream concentration of the solution in contact with a given layer of adsorbent in a column is relatively constant [14]. Then, there is a possibility for the MB molecules to migrate from the external surfaces to the octahedral layers. Therefore, the octahedral layers of MOMD would provide an opportunity to participate in the adsorption of MB molecules. However, MB exhibits an aggregation behaviour, which could block the pore and therefore reduce the intraparticle diffusion coefficient. Therefore, MB diffusion within MOMD can be hampered, as a result of the aggregation of the dye molecules.

From the isotherms studies, the equilibrium adsorption capacities (in terms of milligram of dye per gram of solid) of MB, RB and RY are 320, 419 and 204, respectively. The values of  $q_0$  obtained from the Thomas equation, as shown in Table 5, indicate that the adsorption of dyes on MOMD was in the following order: RB > RY > MB. These column adsorption capacities did not match the equilibrium adsorption capacities. This may be due to the different chemical and physical operating conditions between batch and column experiments. In addition, in the equilibrium adsorption process, the adsorption reached equilibrium in 48 h, while the column adsorption equilibrium was reached

in less than 10 min. However, the fraction of equilibrium below the best conditions was between 4 and 7%. These observations show that flow rate and the column internal diameter are important factors in the adsorption process. Furthermore, these results indicated that intraparticle diffusion acts as the controlling step of the dyes adsorption onto MOMD. It is important to mention here that application of the Thomas model to the experimental data was carried out at  $C_t/C_0$  ratios higher than 0.25 and lower than 0.55 with respect to MB adsorption and higher than 0.40 and lower than 0.70 with respect to RB adsorption. As can be seen in Table 5 RB has the highest equilibrium adsorption capacity onto MOMD and also has the highest column adsorption capacity.

Walker and Weatherley [10] got a poor performance in column studies for the removal of acid dyes using activated carbon. The value of column adsorption capacity was low when compared to the adsorption isotherm capacity. The dissimilarity between the adsorption capacities determined by the two studies might be due to the long service time to reach equilibrium in the adsorption isotherm studies compared with the column experiments, and the solution-phase concentration is continuously decreasing in the isotherm and in the batch systems while that concentration is more constant in the column systems. Therefore, the batch system may provide better interaction between dyes and adsorbent than the column system [23].

The adsorption capacities obtained from the kinetic studies for MB, RB and RY onto MOMD have the same order when compared to the column adsorption capacity. However, in the equilibrium adsorption process, the adsorption reached equilibrium in 120 min, while the column adsorption equilibrium was less than 10 min. This indicates that a microcolumn study is a rapid method to predict the adsorption behaviour in addition to the adsorption parameters.

To conclude, isotherm equilibrium adsorption studies provide useful information on the effectiveness of a dye–adsorbent system. However, the data obtained are generally not applicable under continuous flow conditions where contact time is short for the attainment of equilibrium. Therefore, column studies were performed in order to predict the dye behaviour and the exhaustion period of the column before regeneration.

To make a comparison between the adsorption of MB and RY in small and large columns, one experiment using a large column was carried out and the results are shown in Fig. 10 and Table 7 shows that the column adsorption capacity of MB and RY using a large column are higher by 21 and 47% than that for a small column, respectively. This order coincided with the previous result obtained for a microcolumn with small internal diameter and continuous flow rate.

### 3.3. Multicomponent adsorption

The adsorption of a single dye is not a common process in the textile industries. Textile effluent normally contains multi-species dyes with various concentrations and flow rates. However, adsorption capacities and rates of adsorption may alter upon adsorption of mixtures of dyes. This behaviour should be related to the relative sizes of the molecules being adsorbed, to the relative adsorptive affinities and to the relative concentra-

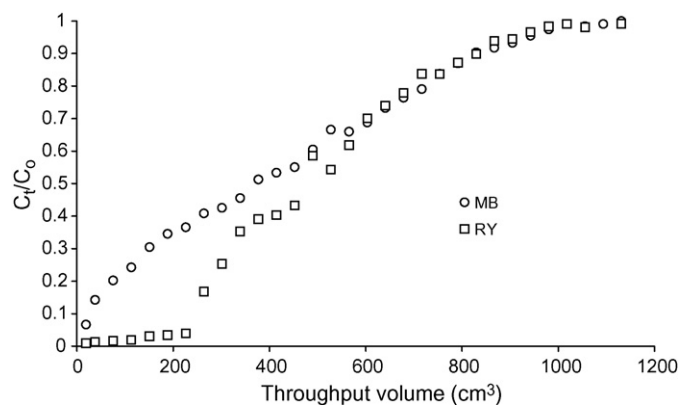


Fig. 10. Breakthrough curve of adsorption of MB and RB onto MOMD using large column. Experimental conditions: mass of MOMD, 1.0 g; flow rate, 3.77 mL/min; pH 2; particle size, 106–250  $\mu\text{m}$ ; temperature, 20 °C; internal diameter, 1.10 cm; initial MB and RY concentration, 46 and 51 mg/L, respectively.

tions of the solutes. Factors that could be influencing mixture adsorption: (i) interactions between dyes in solutions, (ii) the effect of each dye in contributing to the surface charge on the adsorbent, (iii) competition between the difference dyes for the available surface and (iv) the size and structure of individual dye molecules [24]. In fact, little research has been published on the effect of multi-species adsorption in column systems. Competitive adsorption of various initial concentrations of RB and RY onto MOMD using microcolumns was investigated and the results are illustrated in Figs. 11–13. The figures show that the adsorption of RY and RB decreases with the presence of other molecules and the RB adsorption onto MOMD is the highest. This behaviour is expected. Compared to the approach of using information from kinetic and isotherms studies to evaluate the competition behaviour of RB and RY, the adsorption affinity of RB molecules onto MOMD was higher than that for RY molecules. It is reasonable to assume that there is only one adsorption site affecting the adsorption of RB and RY due to the obvious competition in the removal. Chen and Wang [25] studied the competitive adsorption of various metal ions ( $\text{Cu}^{2+}$ ,  $\text{Zn}^{2+}$  and  $\text{Pb}^{2+}$ ) onto granular activated carbon in fixed-bed col-

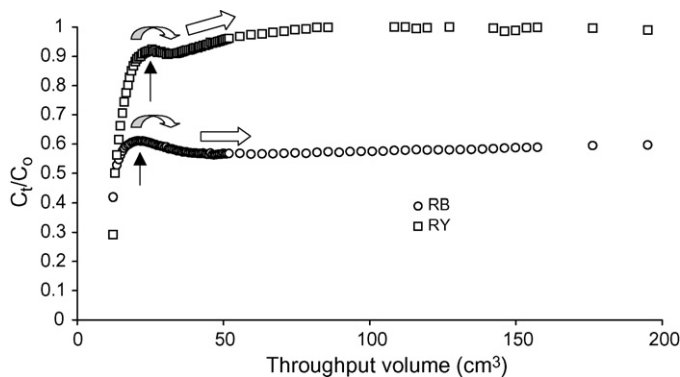


Fig. 11. Breakthrough curve of adsorption of mixture of RB and RY (1:1) onto MOMD using microcolumn. Experimental conditions: mass of MOMD, 0.1 g; flow rate, 3.77 mL/min; pH 2; particle size, 106–250  $\mu\text{m}$ ; temperature, 20 °C; initial RB and RY concentration, 37.0 and 43.9 mg/L, respectively.

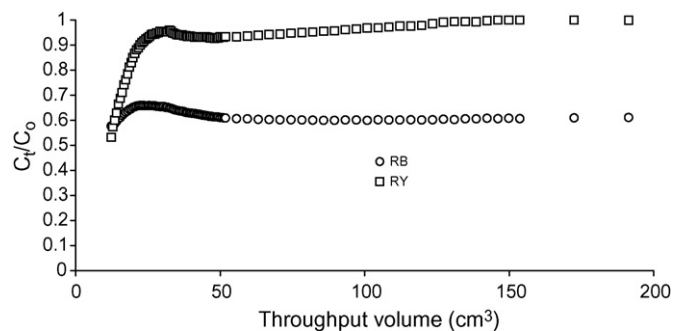


Fig. 12. Breakthrough curve of adsorption of mixture of RB and RY (1:2) onto MOMD using microcolumn. Experimental conditions: mass of MOMD, 0.1 g; flow rate, 3.77 mL/min; pH, 2; particle size, 106–250  $\mu\text{m}$ ; temperature, 20 °C; initial RB and RY concentration, 36.7 and 80.2 mg/L, respectively.

umn. It was noticed that the competition on zinc adsorption by other metal ions (Cu and Cu–Pb) was quite significant. Since the adsorption was less favourable for zinc, other metal ions added competed for adsorption sites with zinc. Consequently, the adsorption of zinc ions decreased as other metal ions were added.

By a quick comparison of the breakthrough curve of the adsorption of single RY and mixture of RY with RB onto MOMD, it is apparent that the presence of the other solutes in the mixture adversely affects the adsorption of the single solute, leading to much more rapid breakthrough and the appearance of an intermediate stage. In this stage, the concentration of RB and RY in the equilibrium dye solution decreased. Figs. 11–13 show the experimental breakthrough curves of mixtures of RB and RY at different proportions. It may be observed that there is a different trend displayed by the adsorption of RY and RB, separately and together. The concentration ratio of RB to RY was (1:1), (2:1) and (1:2). In ratio (1:1), in the intermediate stage of the column operation (the throughput volume 20–50 mL), it is shown that the maximum adsorption of RY onto MOMD is reached after 20 mL of the dye volume treated, while it was after 25 mL for adsorption of RB. Afterwards, the adsorption of RY increased gradually. During this stage, the adsorbed RB or RY molecules were replaced by the incoming RY or RB molecules. Moreover, this intermediate stage was reduced for adsorption of

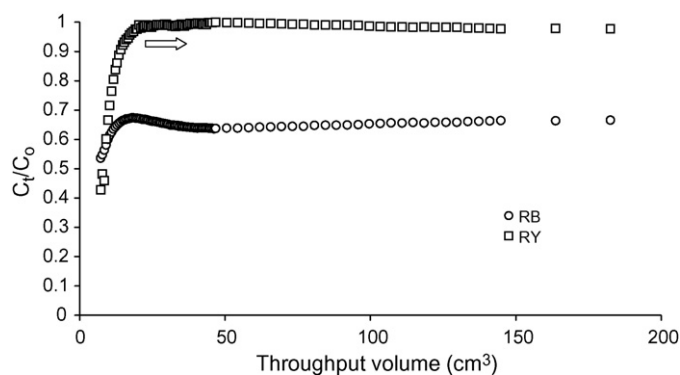


Fig. 13. Breakthrough curve of adsorption of mixture of RB and RY (2:1) onto MOMD using microcolumn. Experimental conditions: mass of MOMD, 0.1 g; flow rate, 3.77 mL/min; pH, 2; particle size, 106–250  $\mu\text{m}$ ; temperature, 20 °C; initial RB and RY concentration, 77.3 and 37.8 mg/L, respectively.

RY if the initial concentration of RY was less than RB concentration. Arrows were drawn to show this behaviour (see Fig. 13). It could be inferred that the RY molecules might influence the adsorption behaviour of RB onto MOMD if the initial RY concentration was equal to or higher than RB concentration. This behaviour was also observed by Chern and Chien [26].

#### 4. Conclusion

Various conclusions could be summarised as follows:

- The adsorption of RY onto MOMD using a microcolumn exhibited a characteristic “S” shape and can be simulated effectively by the Thomas model.
- The adsorption capacity increased as the initial dye concentration increased. This is due to the concentration gradient.
- The increase in the dye uptake capacity with the increase of the adsorbent mass in the column was due to the increase in the surface area of adsorbent, which provided more binding sites for the adsorption.
- The use of high flow rates reduced the time that RY in the solution is in contact with the MOMD, thus allowing less time for adsorption to occur, leading to an early breakthrough of RY.
- A rapid decrease in the column adsorption capacity with an increase in particle size with an average 56% reduction in capacity resulting from an increase in the particle size from 106–250  $\mu\text{m}$  to 250–500  $\mu\text{m}$ .
- The experimental data of RY adsorption onto MOMD correlated well with calculated data using the Thomas equation and the BDST equation. Therefore, it might be concluded that the Thomas equation and the BDST equations can produce accurate prediction for variation of dye concentration, mass of the adsorbent, flow rate and particle size.
- The breakthrough curves obtained for the MB and RB adsorption exhibited different shapes. It was evident that the predominant adsorption mechanism of RB is adsorption in the octahedral layers. This could be explained in that the exhaustion point was not reached (maximum of 75%  $C_0$  effluent concentration after 50 mL). This feature seems to be related to the higher efficiency of MOMD material in removing RB compared with MB or RY.
- Column experiments run at different conditions of particle size, flow rate, dye concentration showed that RY, RB and MB transport in MOMD bed was influenced by mass transfer, mainly intraparticle diffusion. This behaviour may be explained by the layer structure of MOMD.
- The value of column adsorption capacity was low when compared to the adsorption isotherm capacity.

#### References

- [1] F. Li, A. Yuasa, K. Ebie, Y. Azuma, Microcolumn test and model analysis of activated carbon adsorption of dissolved organic matter after pre-coagulation: effects of pH and pore size distribution, *J. Colloid Interface Sci.* 262 (2003) 331–341.
- [2] A.H. Little, *Water supplies and the treatment and disposal of effluents*, Textile Institute Monograph Series, Manchester, 1975.

- [3] M. Al-Ghouti, M.A.M. Khraisheh, M.N.M. Ahmad, S. Allen, Thermodynamic behaviour and the effect of temperature on the removal of dyes from aqueous solution using modified diatomite: a kinetic study, *J. Colloid Interface Sci.* 287 (2005) 6–13.
- [4] M.A.M. Khraisheh, M.A. Al-Ghouti, S.J. Allen, M.N.M. Ahmad, The effect of pH, temperature and molecular size on the removal of dyes from textile effluent using manganese oxides modified diatomite, *Water Environ. Res.* 79 (6) (2004) 51–59.
- [5] W.S. Moore, D.F. Reid, Extraction of radium from natural water using manganese-impregnated acrylic fibres, *J. Geophys. Res.* 78 (1973) 8880–8886.
- [6] M. Khraisheh, A.M. Al-degs, Y.S. Wendy, A.M. McMinn, Remediation of wastewater containing heavy metals using raw and modified diatomite, *Chem. Eng. J.* 99 (2) (2004) 177–184.
- [7] T.N. De Castro Dantas, A.A. Neto, M.C. Moura, Removal of cadmium from aqueous solutions by diatomite with microemulsion, *Water Res.* 35 (9) (2001) 2219–2224.
- [8] G. McKay, H.S.J.R. Blair, Gardner, The adsorption of dyes onto chitin in fixed-bed columns and batch adsorbers, *J. Appl. Polymer Sci.* 29 (1984) 1499–1514.
- [9] L. Conter, R. Knox, *Groundwater Pollution Control*, Lewis, USA, 1986, pp. 96–101.
- [10] G.M. Walker, L.R. Weatherley, Adsorption of acid dyes on the granular activated carbon in fixed-beds, *Water Res.* 31 (8) (1997) 2093–2101.
- [11] J.A. Laszlo, Electrolyte effects on hydrolysed reactive dye binding to quaternize cellulose, *Textile Chemist Colourist* 27 (4) (1996) 25.
- [12] G. McKay, M.J. Bino, Fixed-bed adsorption for the removal of pollutants from water, *Environ. Pollut.* 66 (1990) 33–53.
- [13] Z. Aksu, F. Gönen, Biosorption of phenol by immobilised activated sludge in a continuous packed bed: prediction of breakthrough curves, *Process Biochem.* 39 (2004) 599–613.
- [14] W.J. Weber, *Physicochemical Processes for Water Quality Control*, second ed., John Wiley and sons, New York, 1972.
- [15] V.K.C. Lee, J.F. Porter, G. McKay, Development of fixed-bed adsorber correlation models, *Ind. Eng. Chem. Res.* 39 (2000) 2427–2433.
- [16] D.C.K. Ko, J.F. Porter, G. McKay, Correlation-based approach to the optimisation of fixed-bed sorption units, *Ind. Eng. Chem. Res.* 38 (1999) 4868–4877.
- [17] K.H. Chu, Improved fixed-bed models for metal biosorption, *Chem. Eng. J.* 97 (2004) 233–239.
- [18] Z. Zufadhly, M.D. Mashitah, S. Bhatia, Heavy metals removal in fixed-bed column by the macro fungus *Pycnoporus sanguineus*, *Environ. Pollut.* 112 (2001) 463–470.
- [19] N.K. Lazaridis, T.D. Karapantsios, D. Georgantas, Kinetic analysis for the removal of a reactive dye from aqueous solution onto hydrotalcite by adsorption, *Water Res.* 37 (2003) 3023–3033.
- [20] S. Ouvrard, M.O. Simonnot, P. De Donato, M. Sardin, Diffusion-controlled adsorption of arsenate on natural manganese oxides, *Ind. Eng. Chem. Res.* 41 (2002) 6194–6199.
- [21] C.R. Teixeira Tarley, M.A. Zezzi Arruda, Biosorption of heavy metals using rice milling by-products. Characterisation and application for removal of metals from aqueous effluents, *Chemosphere* 54 (2004) 987–995.
- [22] M.A. Al-Ghouti, M.A.M. Khraisheh, S.J. Allen, M.N. Ahmad, Mechanisms of dye adsorption on modified diatomite, *J. Colloid Interface Sci.*, submitted for publication.
- [23] S. Netpradit, P. Thiravetyan, S. Towpratoon, Evaluation of metal hydroxide sludge for reactive dye adsorption in a fixed-bed column system, *Water Res.* 38 (2004) 70–78.
- [24] S.J. Allen, G. McKay, K.Y. Khader, Multi-component sorption isotherms of basic dyes onto peat, *J. Environ. Pollut.* 52 (1988) 39–53.
- [25] J.P. Chen, X. Wang, Removing copper, zinc, and lead ion by granular activated carbon in pretreated fixed-bed columns, *Sep. Purif. Technol.* 19 (2000) 157–167.
- [26] J.M. Chern, Y.W. Chien, Competitive adsorption of benzoic acid and *p*-nitrophenol onto activated carbon: isotherm and breakthrough curves, *Water Res.* 37 (2003) 2347–2356.